AGRICULTURAL AND ENVIRONMENTAL MODELLING
Publishing data and modelling research objects

Agricultural and Environmental Modelling 8: e184962 (2026)
DOI: 10.3897/aem.8.184962

Formal Model Article Format

Integrating spatial and environmental stressors in a population model of *Folsomia candida* (Collembola, Isotomidae): a Formal Model within ALMaSS framework

Liyan Xie[1], Xiaodong Duan[1], Sarem Norouzi[2], Lis Wollesen de Jonge[2], Christopher J. Topping[1]

1 *Department of Agroecology, Aarhus University, Section for Agricultural Biodiversity, Social-Ecological Systems Simulation Centre, Ole Worms Allé 3, 8000 Aarhus C, Denmark*

2 *Department of Agroecology, Aarhus University, Tjele, Denmark*

Corresponding author: Liyan Xie (liyan.xie@agro.au.dk)

Abstract

Collembola are key soil invertebrates that contribute to decomposition processes and nutrient cycling in agricultural ecosystems. *Folsomia candida*, a parthenogenetic euedaphic species, is widely used as a model organism in ecotoxicological testing, yet population-level responses to environmental stressors in spatially structured landscapes remain poorly understood. We present a formal model of *F. candida* developed using a subpopulation approach within the Animal, Landscape and Man Simulation System (ALMaSS). The model integrates stage-structured population dynamics with spatially explicit landscape processes, incorporating hourly weather data and daily soil moisture dynamics at 10 by 10 m resolution. Growth, development, reproduction, and mortality are driven by temperature, soil moisture, and food quality through empirically parameterised thermal performance curves and dose–response functions fitted to published experimental data. The model explicitly represents egg, juvenile, and adult life stages, with stage transitions and vital rates responding non-linearly to environmental conditions. Soil moisture effects are modelled using a novel integration of ERA5 reanalysis data, soil physical properties, and evapotranspiration to estimate surface soil water potential. Temperature and moisture effects are combined using a limiting-factor approach, reflecting current understanding of physiological constraints. The model is designed for simulations at subpopulation spatial scales of 100 m^2, within landscapes typically 10 km × 10 km, providing a mechanistic framework for exploring *F. candida* population dynamics under realistic environmental heterogeneity in agricultural landscapes. This formal model documentation establishes the theoretical foundation and empirical basis for subsequent model implementation, evaluation, and application to questions in landscape ecology and environmental risk assessment.

Key words: Environmental risk assessment, multiple stressors, population dynamics, population matrix model, spatially explicit model, springtails

OPEN ACCESS

Academic editor: Pavel Stoev
Received: 12 January 2026
Accepted: 6 April 2026
Published: 27 April 2026

Citation: Xie L, Duan X, Norouzi S, de Jonge LW, Topping CJ (2026) Integrating spatial and environmental stressors in a population model of *Folsomia candida* (Collembola, Isotomidae): a Formal Model within ALMaSS framework. Agricultural and Environmental Modelling 8: e184962. https://doi.org/10.3897/aem.8.184962

Copyright: © Liyan Xie et al.
This is an open access article distributed under terms of the Creative Commons Attribution License (Attribution 4.0 International – CC BY 4.0).

Introduction

Soil health is essential for sustaining agricultural productivity, regulating biogeochemical cycles, and maintaining ecosystem stability and resilience. The European Union (EU) has published the EU Soil Strategy for 2030, which identifies soil health as one of its main priorities (European Commission 2021). Healthy soil is supported by both physico-chemical processes and the organisms that live within it. Collembola are among the most abundant soil invertebrates, with an estimated number of 10^5 per square metre in the soil and leaf litter layers of most terrestrial ecosystems (Petersen 1994; Petersen and Luxton 1982). They maintain soil health by contributing to soil nutrient cycling, for example, through the fragmentation of organic matter and the regulation of the microbial community in soil (Fountain and Hopkin 2005; Seastedt 1984; Snider and Butcher 1973), and by serving as prey for other soil organisms such as spiders, mites, millipedes, and ants (Chiverton 1986).

Soil-dwelling Collembola are widely used as model species for assessing the toxicity of chemicals due to their ecological relevance and their distinct exposure pathways compared with earthworms and enchytraeids (OECD 2016). The euedaphic species *Folsomia candida*, which reproduces asexually, has been used as a standard test organism for more than 60 years (Fountain and Hopkin 2005). Numerous studies have described its life-history responses to temperature (Roeben et al. 2023; Snider and Butcher 1973), soil moisture (Holmstrup 2019; Wang et al. 2022), dispersal, and feeding ecology (Johnson and Wellington 1983; van Amelsvoort and Usher 1989), enabling the development of a detailed population model.

Soil-dwelling Collembola depend strongly on moisture, with soil water content playing a role as critical as temperature in shaping their life cycle and activity patterns. To the best of current knowledge, only one population model has explicitly incorporated both temperature and soil moisture: a stage-structured model for *Paronychiurus kimi* (Collembola, Onychiuridae) (Choi et al. 2006). However, that model relies on degree-day theory, which could be improved using thermal performance curves (TPC), and it does not include spatial interaction. An individual-based model for *Folsomia candida* was developed by Meli et al. (2014), in which spatial interactions are explicitly represented (e.g., food and crowd density effects), but soil moisture is not incorporated into life-history processes. Other population models are more limited, typically representing life cycles under constant temperature or without moisture effects, such as Leslie matrix models of *Onychiurus armatus* and *Hypogastrura denticulata* (Longstaff 1977) and degree-day-based models of *Isotoma notahilis* and *P. kimi*, despite the authors noting the importance of moisture (Choi and Ryoo 2003; Diekkrüger and Röske 1995).

To address these limitations, a *Folsomia candida* model was developed within the Animal, Landscape and Man Simulation System (ALMaSS) using the subpopulation modelling approach (Duan and Topping 2024). The model incorporates empirical data on life-stage transitions, reproduction, and mortality across temperature and soil moisture gradients and accounts for spatial interactions such as movement.

This paper follows the formal model format proposed by Topping et al. (2022). A formal model is the first step in a standard modelling cycle, followed by implementation, documentation, evaluation, and testing. Here, the aims and

purpose of the model, the theoretical framework and modelling approach, the mathematical formulation and implementation plan, and a discussion of the data foundations and the model's framing are provided. The 'framing the model' section is dedicated to explicitly defining the domain of the model's applicability, such as excluded biological processes; model boundaries due to the model type or framework; and the implications for use.

Aims and purpose

The *F. candida* model is a stage-structured population model with spatial interaction on a highly detailed landscape simulation. It is developed using the subpopulation approach within the ALMaSS framework. This model aims to represent the species' life cycle under varying environmental conditions in European agricultural landscapes. It enables investigation of *F. candida* population dynamics at the landscape scale, particularly in agricultural systems. It can be further used to study population dynamics in a desired context, for instance, assessing the population-level impacts of agrochemicals usage, such as pesticides and fertilisers, or the impact of different farming practices.

Theoretical framework and modelling approach

The formal model of *F. candida* represents development, reproduction, and mortality using a subpopulation approach within ALMaSS. Details of the ALMaSS framework can be found in Duan and Topping (2024). In brief, the framework consists of the following components:

1. Static landscape elements include habitat, soil type (based on FAO soil texture classification), farm type, and other basic physical properties such as pH, slope, aspect, elevation, and solar radiation.
2. Hourly time-series weather data are input from the ERA5 land reanalysis single levels dataset, including soil and air temperature, humidity, wind speed, wind direction, precipitation, and the volumetric water content at 0–7 cm soil layer.
3. Crop management modelling handles farm practices, crop rotation, pesticide application, and environmental pathways.
4. Vegetation growth modelling handles vegetation growth and flower resources (i.e., pollen and nectar).
5. Species modelling. The majority of species models are built as agent-based models (e.g., Ziółkowska et al. (2023)), while some species models are built using a subpopulation approach (e.g., Thomsen et al. (2024) and the present study).

The modelling of surface soil moisture is a novel addition to ALMaSS. The surface soil moisture is dependent on soil matric potential, which quantifies the energy status of water retained by the soil matrix. Matric potential is the fundamental driver of water flow in unsaturated soils, as water flows from higher to lower potential. Soil matric potential is the proper scientific term used in soil physics, however, it is often called soil water potential in ecotoxicology or ecology. We decided to use soil water potential hereater to be consistent with the references used in ecotoxicology or ecology.

Soil water potential governs water movement and reflects the effort required by soil organisms and plants to extract water (Hillel 2003). It is considered a more universally comparable measure than water content (i.e., mass ratio or relative to water-holding capacity) as it allows comparisons across different soil types. It should be noted that while soil water potential represents a negative sub-atmospheric pressure (i.e., lower potential means more water in soil and represents as a larger negative number), it is commonly expressed on a positive scale with a minus sign in front of the units.

Due to challenges associated with the direct estimation of soil water potential, the surface volumetric water content ($\theta_{surface}$) and convert it to soil water potential (i.e., -10^{pF}, where pF is the logarithm of the absolute value of soil water potential in centimetres of water (i.e., pF = log10|h|) using soil water retention curves (SWRC). The SWRC is a fundamental soil property that defines the relationship between water content and soil water potential in soil. The SWRC varies among soil types and can be estimated using soil pedotransfer functions based on readily available soil properties. In this study, the physics-informed pedotransfer function of Norouzi et al. (2025) is used, which estimates the entire SWRC from saturation to oven-dry conditions based on five soil properties: sand, silt, clay, organic carbon content, and bulk density. This model was trained on a comprehensive dataset consisting of 4,200 soil samples well distributed across Denmark.

Landscape is represented as polygons in ALMaSS. Landscape polygons contain soil-type information, and for each soil type, sand, silt, and clay percentages, organic carbon content, and bulk density are retrieved via the soil mapping database integrated in ALMaSS (Adhikari et al. 2014; Adhikari et al. 2013; Adhikari et al. 2014). These inputs are then fed into Norouzi et al.'s (2025) pedotransfer function to obtain the corresponding SWRC for each soil sample (see details in Suppl. material 1: table S1, fig. S1).

Hourly volumetric water content for the 0–7 cm soil layer ($\theta_{surface}$) is obtained from the ERA5 reanalysis single-level dataset (Hersbach et al. 2023). The native spatial resolution of the dataset (0.25°, approximately 28 km) exceeds the typical ALMaSS landscape window (10 km × 10 km). In ALMaSS, landscape attributes such as slope and elevation are represented at the polygon scale. Therefore, $\theta_{surface}$ is redistributed to each polygon based on slope, elevation, and evapotranspiration. This redistributed soil moisture estimate is applied consistently throughout the model.

The slope (S) is expressed in degrees and ranges from 0 to 90, with higher numbers indicating steeper terrain. $S_{polygon}$ denotes the slope at the polygon scale, and S_{total} represents the aggregated slope across all polygons within a landscape. Elevation (H) varies by location and may take negative values where terrain lies below the sea level, with lower values corresponding to lower-lying areas in the landscape. $H_{polygon}$ denotes polygon-level elevation, H_{lowest} the minimum elevation within the landscape, and H_{total} the aggregated elevation across all polygons within a landscape. As water accumulates in flatter and lower-lying areas, terrain slope and elevation are used to redistribute soil moisture accordingly. Volumetric evapotranspiration (θ_{evpt} ,m^3/m^3) negatively relates to the $\theta_{surface}$ The volumetric water content at the polygon level (Refined $\theta_{surface_polygon}$) is defined as follows:

$$\begin{cases} Refined\theta_{surface_polygon} = \theta_{surface} * \left(1 - \frac{S_{polygon}}{S_{total}}\right) * \left(\frac{H_{polygon} + |H_{lowest}|}{|H_{lowest}| * H_{total}}\right) - \theta_{evpt}, & \text{if} \quad H_{lowest} < 0 \\ Refined\theta_{surface_polygon} = \theta_{surface} * \left(1 - \frac{S_{polygon}}{S_{total}}\right) * \left(\frac{H_{polygon}}{H_{total}}\right) - \theta_{evpt}, & \text{if} \quad H_{lowest} > 0 \end{cases} \tag{1}$$

Evapotranspiration (ET) depends on crop types and weather (Allen et al. 1998). It is estimated as a multiplication of K_c (crop coefficient) and ET_0 (reference crop evapotranspiration) using a crop coefficient approach.

$$ET = K_c * ET_0 \tag{2}$$

Crop coefficient (K_c) holds an exponential relationship with leaf area index (LAI) (Al-Kaisi et al. 1989; Jia and Wang 2021). We generalise the relationship between K_c and LAI in the form of Equation 3, where parameters a, b, and c are crop dependent. If there is available data on measured K_c and measured LAI, these three parameters will be easily fitted. For example, values of these three parameters for maize are 1.059, −1, and −0.488, and for apple orchard are 0, 0.1141 and 1.0665. If such data are not available for the interest of the crop, default values of 1.1, −1.1 and −1.5 will be used as parameters a, b, and c in accordance with the Wisconsin irrigation scheduler workbook (Nielmeyer 2022).

$$K_c = a + b * e^{c*LAI} \tag{3}$$

Reference crop evapotranspiration (ET_0) can be calculated with the Penman–Monteith equation (Allen et al. 1998), but here we will use an average value of ET_0 based on the agroclimatic regions. For example, Denmark is recognised as a temperate region with characteristics of humid and sub-humid (Danish Agriculture Food Council 2000), the average ET_0 when the temperature is lower than 10 °C is 1.5 mm/day, from 10 °C to 30 °C is 3 mm/day, and above 30 °C is 5.5 mm/day (Allen et al. 1998). Combining Equations 2 and 3, we have:

$$ET = \begin{cases} \left(1.1 - 1.1\mathrm{e}^{-1.5LAI}\right) \times 1.5, & \text{if} \quad T < 10^{\circ}\mathrm{C} \\ \left(1.1 - 1.1\mathrm{e}^{-1.5LAI}\right) \times 3.0, & \text{if} \quad 10^{\circ}\mathrm{C} \leq T \leq 30^{\circ}\mathrm{C} \\ \left(1.1 - 1.1\mathrm{e}^{-1.5LAI}\right) \times 5.5, & \text{if} \quad T > 30^{\circ}\mathrm{C} \end{cases} \tag{4}$$

Covert evapotranspiration into a volumetric unit.

$$\theta_{evpt} = \left(\frac{ET}{1000} * A_{polygon}\right) / \left(A_{polygon} * 0.07m\right) \tag{5}$$

Overview of processes

The structure of the model encompasses three key life history components of *F. candida*: growth and development, reproduction, and mortality. Growth and development are influenced by temperature, soil moisture, and the food conditions (i.e., the availability and quality of food resources). Reproduction occurs parthenogenetically and is determined by temperature and soil moisture conditions. Mortality is influenced by temperature, soil moisture, and predation. These components and their associated environmental drivers are described in detail in the sections below.

Growth and development

Folsomia candida is a euedaphic collembolan species that inhabits the upper soil layers, typically within the top 5 cm of the soil profile. Its life cycle comprises three stages: egg, juvenile, and adult. Under suitable temperature and soil moisture conditions, eggs hatch at age day 0, and the age of each individual increases by one day thereafter. Both hatching success and hatching time are influenced by temperature and soil moisture. After hatching, juveniles begin feeding immediately. As they consume sufficient food, they undergo successive moults, each marking the transition to the next instar. Following six moults, juveniles reach sexual maturity and become adults. Adults continue moulting throughout life but without further morphological change.

Temperature, soil moisture, and food conditions determine growth and development in animals. However, the interactions among these factors remain poorly understood. It is therefore assumed that the total development rate ($r_{dev,\,total}$) at each life stage is limited by the most restrictive of the temperature-dependent and soil-moisture-dependent development rates. This reflects the principle that favourable moisture cannot compensate for temperatures that already impose strong physiological constraints. The plausibility of this assumption was evaluated by visualising development rates across all combinations of temperature and soil moisture (Suppl. material 1: figs S2–S4). The limiting development rate is subsequently scaled by the food score, as expressed in Equation 6.

$$r_{dev,total} = food\ score \times min\left(r_{dev,temperature}, r_{dev,soil\ moisture}\right) \tag{6}$$

Temperature

The development rate of each life stage is characterised using a thermal performance curve based on the Lobry–Rosso–Flandrois model (LRF) (Rosso et al. 1993). The LRF curve describes the relationship between temperature (T) and biological development rate (r), defined in Equation 7. The curve is characterised by four key parameters: the thermal optimum (t_{opt}) at which the performance rate r is maximal (r_{max}), and maximum temperature (t_{max}), optimal temperature and minimum temperature (t_{min}).

$$r = r_{max} \times \frac{(T - t_{max}) \times (T - t_{min})^2}{(t_{opt} - t_{min}) \times ((t_{opt} - t_{min}) \times (T - t_{opt}) - (t_{opt} - t_{max}) \times (t_{opt} + t_{min} - 2 \times T))} \tag{7}$$

Hatching time from 4 to 24 °C was compiled from Fountain and Hopkin (2005), Holmstrup (2019), and Roeben (2023). Eggs fail to hatch above 28 °C, and the optimal temperature for hatching success is 21 °C (Fountain and Hopkin 2005). Development rate from oviposition to hatching ($r_{egg \rightarrow juvenile}$) was calculated as the reciprocal of hatching time (d^{-1}).

The onset of oviposition marks the attainment of sexual maturity. Time to first oviposition across 4 to 26 °C was collected from published studies (de Lima et al. 2021; Fountain and Hopkin 2005; Holmstrup 1994; Roeben et al. 2023; Snider and Butcher 1973). As no reproduction occurs at 0 °C or 30 °C, the juvenile-to-adult development rate ($r_{juvenile \rightarrow adult}$) was set to zero at those extremes. Otherwise, it was calculated as the reciprocal of the time to first oviposition (in days).

The end of the reproductive period corresponds to the cessation of egg-laying. The time to last oviposition between 4 and 26.6 °C was obtained from Grégoire-Wibo (1983) and Roeben et al. (2023), who used comparable methods. Reproduction does not occur at 0 °C or 30 °C, so the adult-to post-productive development rate ($r_{adult \rightarrow post\text{-}reproduction}$) was set to zero at these temperatures and elsewhere calculated as one divided by the interval between first and last oviposition (in days) (Fig. 1). Parameter estimates for the LRF curves are summarised in Table 1.

Table 1. Fitted parameters of LRF thermal performance curve for each life stage transition.

	r_{max} (per day)	t_{max} (°C)	t_{opt} (°C)	t_{min} (°C)
$r_{egg \rightarrow juvenile}$	0.127	28.0	26.8	-5.15
$r_{juvenile \rightarrow adult}$	0.0561	30.0	21.7	-5.53
$r_{adult \rightarrow post\text{-}reproduction}$	0.0109	30.0	30	-0.661

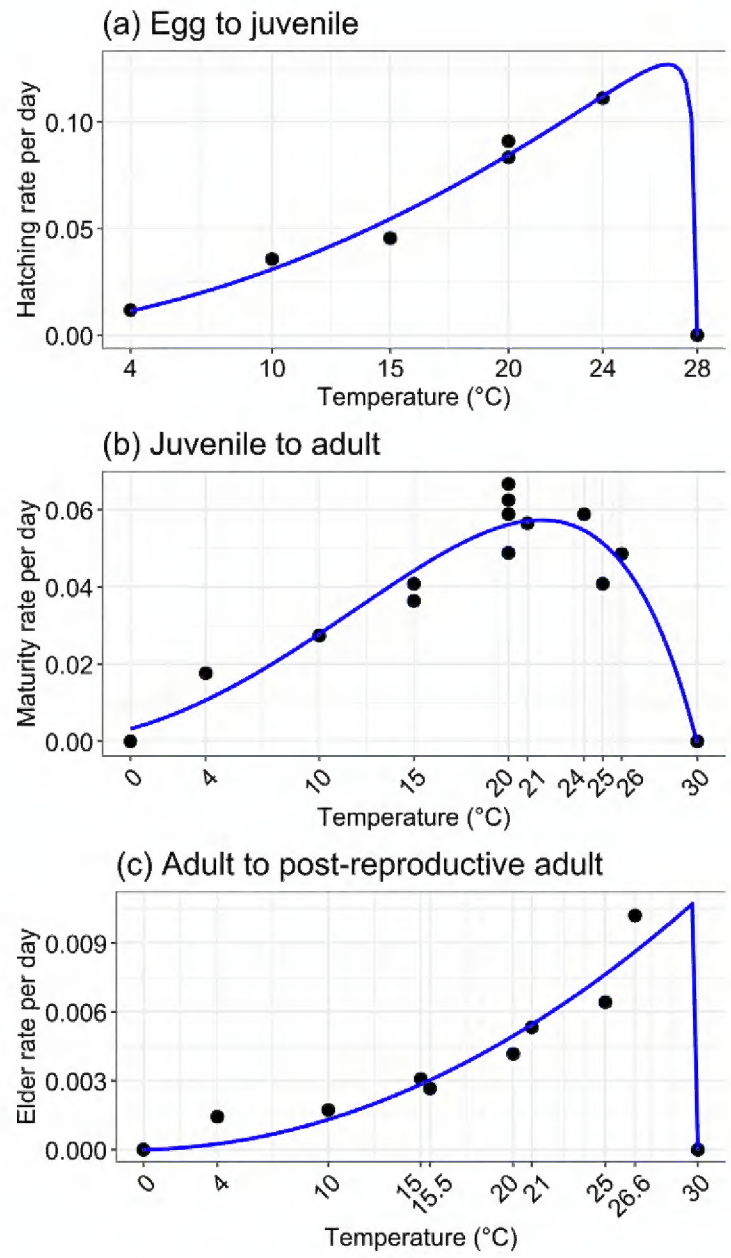

Figure 1. Development rate across a range of temperatures for life stage transition (**a**) from egg to juvenile; (**b**) from juvenile to adult; and (**c**) from adult to post-reproductive adult. Data is presented as a mean value, as the original paper suggests, and blue solid lines show the fitted LRF model.

Soil moisture

Collembola prefer moist habitats, and euedaphic species are particularly sensitive to soil moisture. At constant optimal temperature, development generally ceases below a moisture threshold. A three-phase model, reparameterised for both eggs to juveniles and juveniles to adults, was constructed to capture *F. candida*'s response to soil moisture.

A three-phase model (Equation 8) fitted to data from Holmstrup (2019) describes the daily development rate from egg to hatching across soil moisture conditions. Because available data for development from egg to juvenile are limited, a linear relationship between soil moisture and juvenile-to-adult development is assumed. The lower bound of the *x*-domain is defined as zero, which also applies to other equations involving soil water potential. Based on the data, a constant rate of 0.084 when soil water potential ranges from 0 to 0.11 MPa is used. The dataset and model fitting process can be found in Section 7.

$$rate_{egg \rightarrow juvenile} = \begin{cases} 0.084, 0 \leq x < 0.11 - MPa \\ -0.0153x + 0.0873, 0.11 \leq x < 1.88 - MPa \\ 0, x \geq 1.88 - MPa \end{cases} \quad (8)$$

A similar approach is used to model the development of *F. candida* from juvenile to adult under varying soil moisture conditions. Due to limited available data, it is assumed that the relation between soil moisture and development from juvenile to adult is also linear. A full life-cycle experiment conducted under three distinct soil moisture conditions contributed to the model fitting (Xie 2023). Additional studies indicate that cessation of reproduction beyond 96 kPa (Wang et al. 2022), so the development rate from juvenile to adult is set to zero above this threshold.

$$rate_{juvenile \rightarrow adult} = \begin{cases} 0.0520, 0 \leq \mathbf{x} < 0.00262 - MPa \\ -0.427x + 0.0531, \quad 0.00262 \leq \mathbf{x} < 0.096 - MPa \\ 0, \quad \mathbf{x} \geq 0.096 - MPa \end{cases} \quad (9)$$

Data on the time to last oviposition at different soil moisture levels are unavailable. Therefore, a constant development rate ($rate_{adult \rightarrow post\text{-}reproduction}$) of 0.052 per day is adopted from $rate_{juvenile \rightarrow adult}$ for 0 to 0.096 -MPa, with the rate set to zero under drier conditions.

Food availability and quality

Food availability and quality influence the growth, development, and reproduction of *F. candida* and therefore shape its population dynamics (Booth and Anderson 1979; van Amelsvoort and Usher 1989). Common food sources for *F. candida* are fungus spores, organic matter, and plant litter (Bakonyi 1989; Kaneda and Kaneko 2002; Ponge 1991; Rusek 1998). The availability of these sources depends strongly on temperature and soil moisture, as they control microbial metabolism, fungal growth, and carbon mineralisation (Curtin et al. 2012; Talley et al. 2002). Food availability (*A*) is the product of a temperature response (*T*) and soil moisture response (*SM*) (Equations 10–12).

$$A = A_T \times A_{SM} \quad (10)$$

$$A_T = \begin{cases} 1, 20°\mathrm{C} \leq T \leq 30°\mathrm{C} \\ 0.6, 5°\mathrm{C} \leq T < 20°\mathrm{C} \\ 0.2, T < 5°\mathrm{C} \quad \text{or} \quad T > 30°\mathrm{C} \end{cases} \quad (11)$$

$$A_{SM} = \begin{cases} 1, & soil\ moisture < 0.005 - MPa \\ 0.6, & 0.005 \leq soil\ moisture < 0.72 - MPa \\ 0.2, & soil\ moisture \geq 0.72 - MPa \end{cases} \quad (12)$$

Depending on food sources, food quality (q_i) is assigned a weight (w_i) reflecting its relative contribution to the overall diet quality. Nutritional quality relative to Baker's yeast (q_y)), which is 1 in the laboratory baseline (van Amelsvoort and Usher 1989). Fungus spores (q_{FS}) and organic matter (q_{OM}) are assigned as 0.6, and plant litter (q_{PL}) is 0.2. These scores are adapted based on the previous studies where Baker's yeast-fed *F. candida* gave the best results in reproduction and growth, indicating it is a good quality food source (van Amelsvoort and Usher 1989), whereas fungus spores show intermediate results in moulting rate and egg-laying rate compared with yeast-fed springtail (Booth and Anderson 1979). Plant litter shows low food quality (low nutrition), although it depends on plant species (van Amelsvoort and Usher 1989); it is assumed that all plant litter has lower food quality and lower nutrition than fungus spores and yeast. A dimensionless food score is introduced to integrate availability and quality in this model.

$$\text{Food score} = \sum_i A * w_i * q_i \quad (13)$$

with weights w_i summing to one, and *i* denotes the food type (Baker's yeast, fungus spores, organic matter, or plant litter).

Reproduction

Folsomia candida reproduces via parthenogenesis, with males rarely present in laboratory culture or the field. Once juveniles reach sexual maturity, typically at the sixth instar, females begin laying eggs in batches. Batch size depends on the animal's age, food availability, and environmental conditions (Booth and Anderson 1979; Roeben et al. 2023; Snider and Butcher 1973; van Amelsvoort and Usher 1989). Age-specific variation in batch size, although documented, is not incorporated in the present model due to limited data across environmental gradients.

In this model, the total reproduction rate ($r_{rep,total}$) is determined by temperature, soil moisture, and food conditions. These components are modelled independently, and the minimum of the temperature-driven and moisture-driven reproduction rates is taken as the total reproductive rate rate (Equation 14). The plausibility of this assumption was evaluated (see Suppl. material 1: fig. S5).

$$r_{rep,total} = \text{Food score} \times min\left(rate_{rep,temperature}, rate_{rep,soil\ moisture}\right) \quad (14)$$

Temperature

Total fecundity, defined as the lifetime number of eggs laid per female, varies with temperature. Although oviposition rate typically increases early in the reproductive period and declines towards its end (Snider and Butcher 1973), the available data are limited to only two temperatures. Con-

sequently, a constant daily reproduction rate is assumed at each temperature. An LRF thermal performance curve was fitted to fecundity data from C. Grégoire-Wibo (1983), Roeben et al. (2023), Snider and Butcher (1973). The daily reproduction rate is calculated as total fecundity divided by the total number of reproductive days. Fitted parameters are listed in Table 2, and the fitted curve is illustrated in Fig. 2.

Table 2. Fitted parameters of the LRF thermal performance curve for the reproduction rate.

	r_{max} (per day)	t_{max} (°C)	t_{opt} (°C)	t_{min} (°C)
reproduction rate$_{temperature}$	5.58	29.3	18.8	1.51

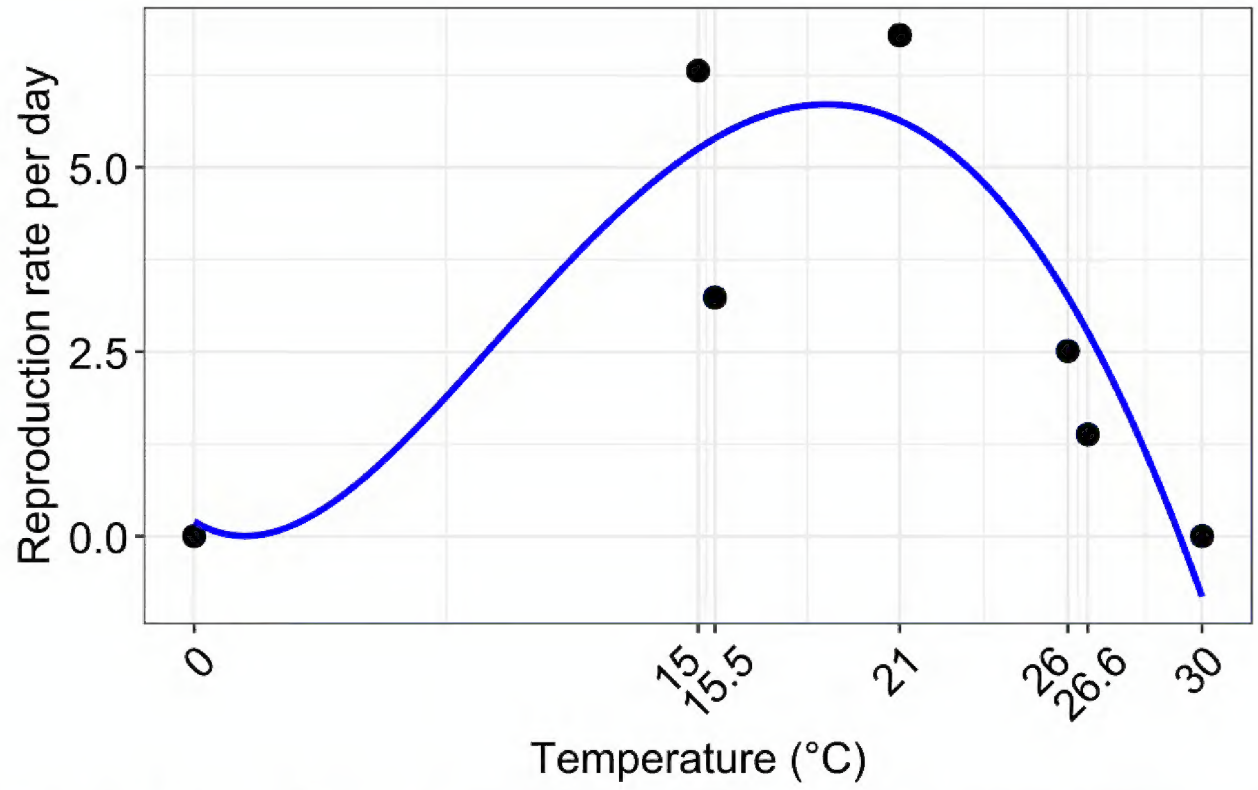

Figure 2. The fitted LRF thermal performance curve for reproductive rate. Reproduction rate calculated as total fecundity per female divided by total reproductive days. Data is presented as a mean value, as the original paper suggests, and the blue solid line shows the fitted model.

Soil moisture

Reproduction is strongly influenced by soil moisture. Empirical studies show that egg production declines under even moderate drought stress and ceases completely under medium-dry conditions (Wang et al. 2022). However, few studies report actual egg counts; most report the number of juveniles. To avoid bias, only studies that report actual egg counts were used to calculate the reproduction rate as a function of soil moisture.

Reproduction rate ($r_{rep,soil\ moisture}$) is calculated as the number of eggs produced during the experimental period divided by the number of reproductive days. Because experimental duration constrains observed reproductive periods, raw reproduction rates tend to be overestimated. A correction factor (a) was therefore applied by comparing the temperature-derived maximum rate (i.e., $a = r_{max_temperature}/r_{rep,\ soil\ moisture} = 5.58/12.16 = 0.46$). The data used to construct the reproduction function were obtained from an experiment conducted at 20 °C (Xie 2023). The model is structured as a three-phase model to capture key moisture-dependent dynamics, defined as follows.

$$r_{rep,soil\ moiture} = \begin{cases} 12.16 * a, 0 \leq x < 0.00262 - MPa, \text{where} \quad a = 0.46 \\ (-131.69\text{x} + 12.51) * a, 0.00262 \leq x < 0.096 - MPa, \text{where} \quad a = 0.46 \\ 0, x \geq 0.096 - MPa \end{cases} \tag{15}$$

Mortality

Mortality in the model arises from three components: temperature stress, soil-moisture stress, and predation. The total daily mortality rate is assumed to be the sum of these independent components (additive mortality). Mortality is recalculated as the death rate per day for each life stage. Mortality is expressed as a daily death-rate increment; individuals die when their accumulated death value reaches one.

Temperature

Temperature-induced mortality differs among life stages. Egg mortality (hatchability) at different temperatures reflects the viability of eggs incubated under those conditions. While animal age can influence hatchability, available data are limited to only three temperatures, which is insufficient to establish meaningful patterns. As a result, the effect of animal age on hatchability is excluded from the model. Hatchability is modelled using a three-parameter log-logistic function (Equation 16).

$$y = c + \frac{1 - c}{1 + \exp(b(\log(x) - \log(e)))} \tag{16}$$

Parameters *b*, *c* and *e* are the slope, lower limit of the response variable, and median lethal temperature, respectively. Data used to fit this model combines various studies, including Fountain and Hopkin (2005), Jensen et al. (2020), Snider and Butcher (1973), Xie et al. (2024), and Xie (2023). The daily death rate was calculated as one minus hatchability divided by hatching time, where hatching time was estimated from the LRF thermal performance curve for egg-to-juvenile development (Equation 1; Table 1).

At excessively high temperatures, juveniles fail to reach adulthood; mortality is set to the inverse of lifespan (i.e., one divided by the number of days lived). Under optimal temperatures, juveniles reach maturity without mortality, so the daily death rate is zero. At intermediate temperatures that produce partial survival, the daily death rate is calculated as the proportion of individuals that died divided by the time to first oviposition among survivors. Two distinct temperature–mortality relationships emerged for temperatures below 20 °C and above 20 °C (Roeben et al. 2023; Snider and Butcher 1973; Wehrli et al. 2024). Each was fitted separately using quadratic (Equation 16) or log-logistic forms (Equation 17).

$$y = ax^2 + bx + c \tag{17}$$

The adult mortality rate is calculated as the inverse of the time interval between the first oviposition and death. Data from multiple studies were fitted to a log-logistic temperature–mortality function (Roeben et al. 2023; Snider and Butcher 1973; Wehrli et al. 2024).

The functions and their fitted parameters for each life stage are summarised in Table 3 and visualised in Figs 3 to 5.

Table 3. Fitted functions on the effect of temperature on mortality at each life stage.

Life stage	Functions	Fitted functions
Egg	Log-logistic	$y = 0.0131 + \frac{0.9869}{1 + \exp(-131.25(\log(x) - \log(26.76)))}$
Juvenile	Quadratic and Log-logistic	$y = \begin{cases} -7.98 \times 10^{-6}x^2 + 1.36 \times 10^{-5}x + 2.99 \times 10^{-3}, x < 20°C \\ 0.0047 + \frac{0.9953}{1+\exp(-232(\log(x)-\log(31.52)))}, x \geq 20°C \end{cases}$
Adult	Log-logistic	$y = -0.000747 + \frac{0.9993}{1 + \exp(-237.83(\log(x) - \log(31.40)))}$

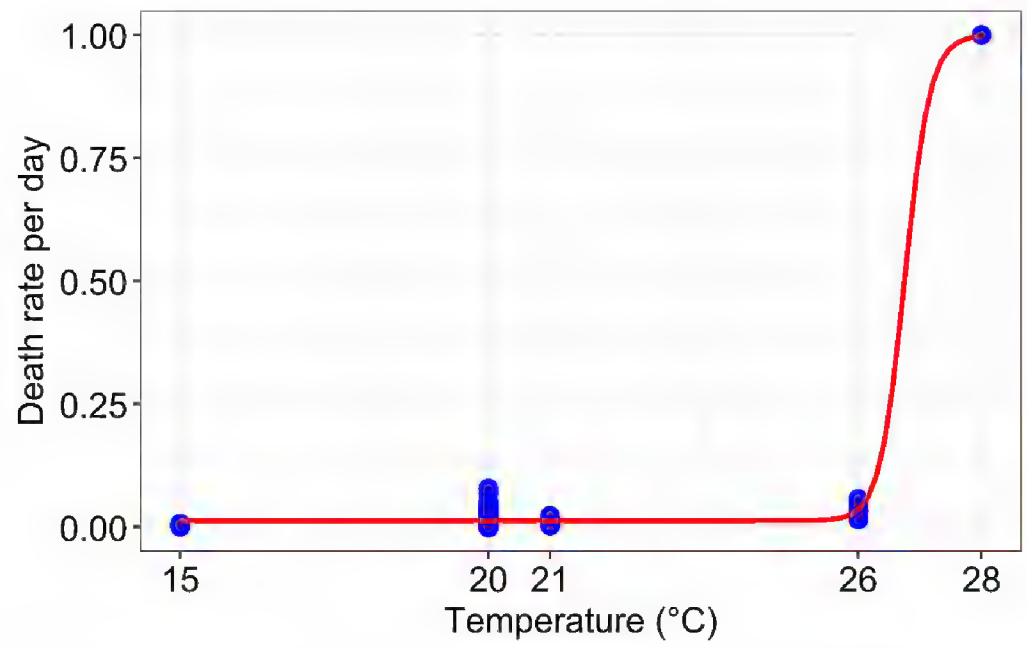

Figure 3. The fitted three-parameter log-logistic function for death rate per day versus temperature at the egg stage. Data is presented as an original data point (blue solid dot). For 15, 21, and 26 °C, the hatchability is from different instars (Snider and Butcher 1973). The red solid line shows the fitted model.

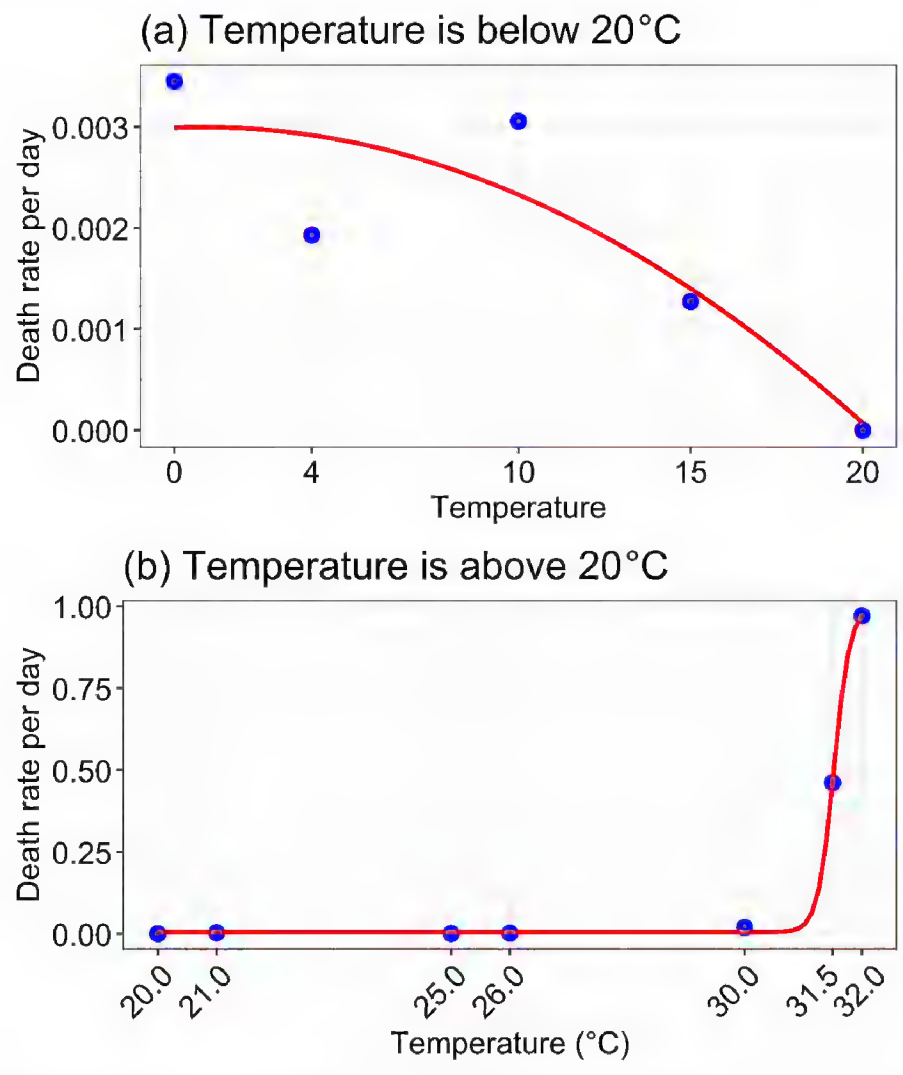

Figure 4. The fitted models of temperature effect on death rate at juvenile phases (**a**) when temperature is below 20 °C and (**b**) when temperature is above 20 °C (incl. 20 °C). Data is presented as a mean value, and the red solid line shows the fitted model.

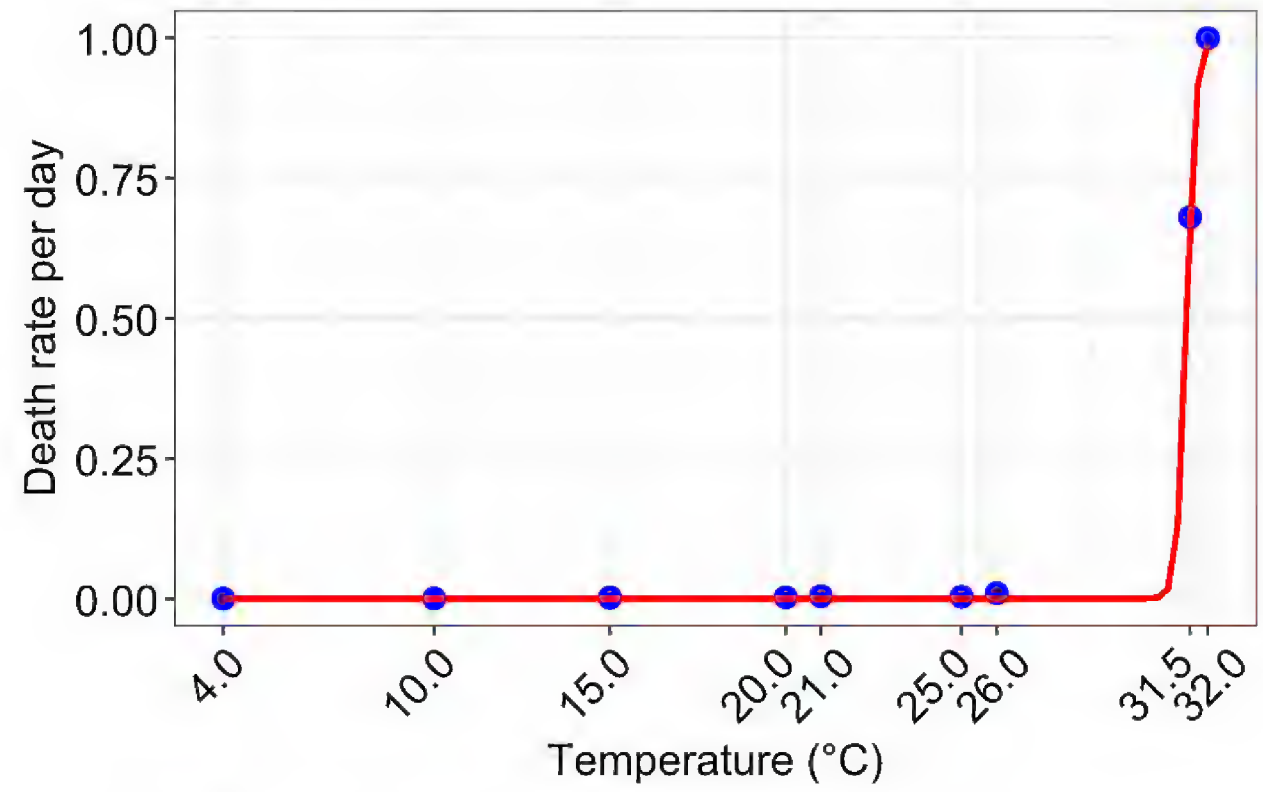

Figure 5. The fitted three-parameter log-logistic function for death rate per day versus temperature at the adult stage. Data is presented as a mean value, and the red solid line shows the fitted model.

Soil moisture

Soil moisture-induced mortality is modelled using log-logistic functions for eggs and adults (Equation 16) and by adapting the function from the egg stage for the juvenile stage due to lack of data. Mean values from Fig. 3 in the paper of Holmstrup (2019) were used to fit the egg mortality function.

Empirical data on juvenile mortality under varying soil moisture are limited. Only one life-cycle experiment is available (Xie 2023), which showed complete juvenile survival between 0.00262 and 0.0147 MPa. Mortality is therefore set to zero within this range. For drier conditions, the egg-stage moisture–mortality function is used as a conservative estimate, recognising that juveniles are typically more drought-tolerant than eggs.

For adults, data on soil moisture on *F. candida* covering its whole life do not exist to the best of current knowledge. Mortality data from chronic exposure studies (i.e., exposure duration over one week), in which animals were exposed to varied drought at the adult stage and adult mortality was measured only at the end of the experimental period (Wang et al. 2023; Wang et al. 2022). The daily death rate was therefore calculated as mortality divided by exposure duration. A log-logistic curve was fitted to these data.

The fitted parameters are summarised in Table 4 and visualised in Figs 6 to 7.

Table 4. Fitted functions on the effect of soil moisture conditions on mortality at each life stage.

Life stage	Function	Fitted functions
Egg	Log-logistic	$y = 0.044 + \frac{0.956}{1 + \exp(-51.3(\log(x) - \log(1.34)))}$
Juvenile	Adapted from the egg stage	$y = \begin{cases} 0, x \leq 0.0147 - \mathrm{MPa} \\ 0.044 + \frac{0.956}{1+\exp(-51.3(\log(x)-\log(1.34)))}, x > 0.0147 - \mathrm{MPa} \end{cases}$
Adult	Log-logistic	$y = 0.00016 + \frac{0.99984}{1 + \exp(-1.62(\log(x) - \log(16.07)))}$

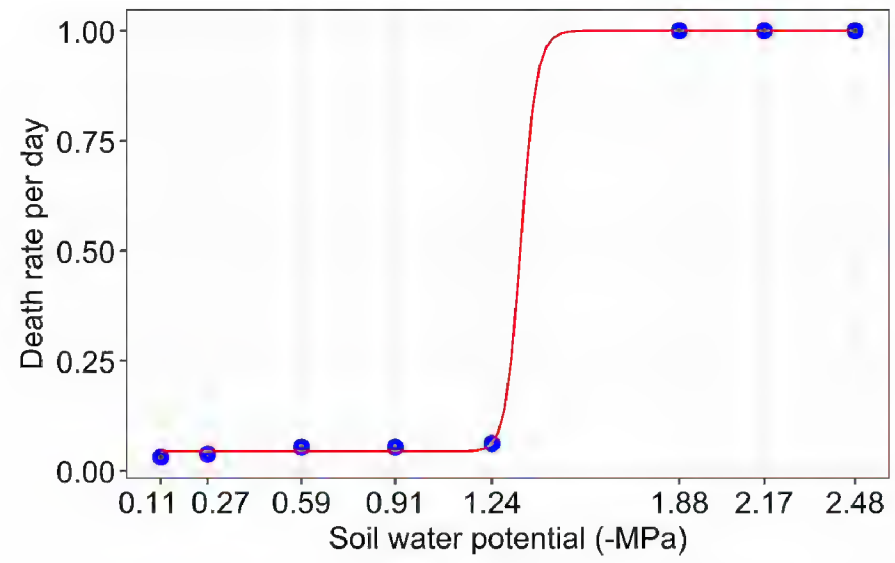

Figure 6. The fitted three-parameter log-logistic function for death rate per day versus soil moisture at the egg stage. Data is presented as a mean value, and the red solid line represents the fitted model.

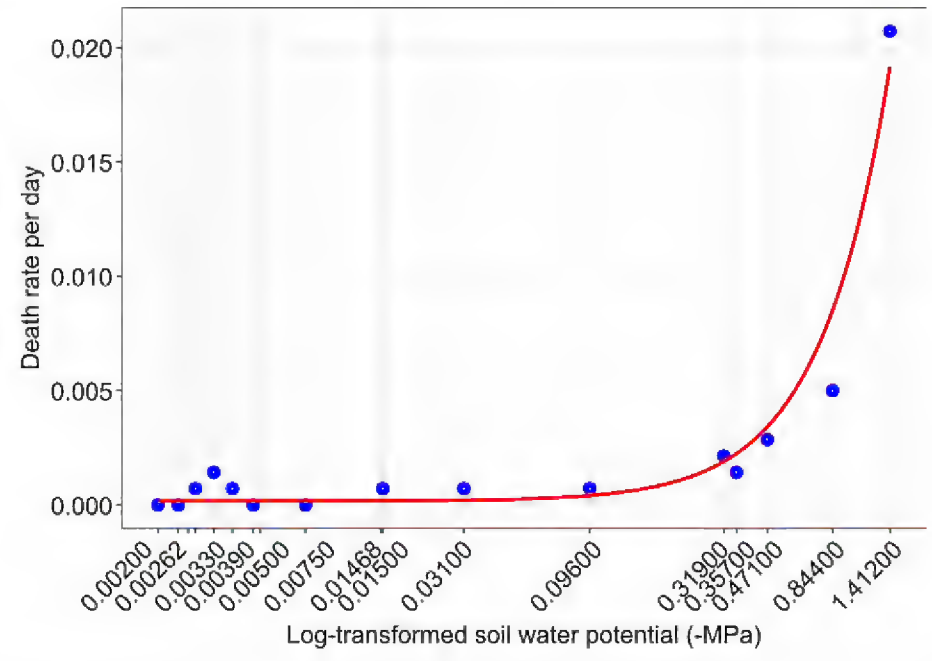

Figure 7. The fitted three-parameter log-logistic function for death rate per day versus soil moisture at the adult stage. Data is presented as the mean. The red solid line shows the fitted model. The black circles are data points that are used to fit the model.

Predation

Collembola form a key prey group for numerous soil predators, including spiders and centipedes (Chiverton 1986; Frampton 1988). Due to insufficient data to parameterise mechanistic predator–prey dynamics, predation is modelled as a fixed percentage of individuals removed daily from each life stage. This predation fraction will be estimated during model calibration. Although predation likely varies across habitats and seasons, a constant rate is applied in the present version due to a lack of data.

Dispersal

Euedaphic species, especially parthenogenetic species, have poor dispersal capacity. Becoming parthenogenetic instead of dispersing might be the strategy for them to tackle the changing environment (Ponge 2020). Therefore, dispersal is modelled simply. Juvenile *F. candida* is largely sedentary, and the foraging range of adults scales with body size, with a 2 mm adult typically moving up to 20 cm (Johnson and Wellington 1983). For simplicity, only adults disperse in the model. Dispersal occurs by random movement into the eight surrounding grid cells. Dispersal of adults only occurs when population density is over

10^5 per square metre (Petersen 1994; Petersen and Luxton 1982) or the food score is less than 0.008 (assuming plant litter is the only food source and food availability is lowest, which is 0.04).

Discussion

Handling of missing soil water potential data

Studies of temperature effects on *Folsomia candida* often only mentioned that the experiment carried under controlled humidity (i.e., air humidity). In soil-based experiments, moisture is frequently reported as gravimetric or volumetric water content rather than soil water potential. In other cases, *F. candida* is reared on moist plaster, where the moisture condition is reported as "water is added regularly to maintain saturation". When water-potential data are missing, assumptions must be made. We assumed that animals experienced optimal soil water potential (approximately 1.8 -kPa) in cases mentioned above. This approach ensures consistency across datasets used for model parameterisation.

Integration of temperature and soil moisture effects

Temperature and soil moisture jointly shape physiological performance in soil invertebrates. In this model, the combined effects of temperature and moisture are represented using a limiting-factor approach in which the realised rate is the minimum of the temperature-driven and moisture-driven rates. This reflects the idea that extreme drought cannot be compensated for by optimal temperature, and vice versa. The true interaction between temperature and soil moisture in *F. candida* remains poorly quantified. Potential synergistic, antagonistic, or additive effects are not well resolved in the literature. In the absence of mechanistic data, the minimum-rate approach provides a conservative approximation while avoiding structurally unjustified interaction terms.

Response to extreme temperature

The model predicts complete mortality when soil temperature exceeds approximately 32 °C, whereas soil moisture exerts a comparatively minor influence within most of its range. However, natural soils exhibit substantial microclimatic heterogeneity, and individual springtails may occupy cooler or moister microsites within soil aggregates or pore spaces. Microhabitats may buffer exposure to temperature extremes, allowing survival even when surface or bulk soil temperatures exceed lethal thresholds.

Explicit representation of microclimatic could improve biological realism but would require spatial resolutions far finer than the 1 m^2 grid used in ALMaSS. While desirable for future mechanistic studies of soil arthropod thermal ecology, such fine-scale resolution is beyond the scope of landscape-scale modelling.

Stage-specific daily death rate under temperature and soil moisture

Differences in available data between temperature and soil moisture effects result in distinct approaches for modelling the daily death rate for juveniles

and adults. The juvenile daily death rate derives from full life-cycle experiments. Under excessively high temperatures, juveniles never reach adulthood, and the daily death rate is defined as the inverse of lifespan. Under optimal temperatures, all juveniles mature, and the daily death rate is zero. Intermediate temperatures yield partial mortality, calculated as deaths divided by time to first oviposition among survivors. The soil-moisture-dependent daily death rate for juveniles is based on sparse data; complete survival is observed between −0.00262 and −0.0147 MPa (Xie 2023). Mortality is therefore assumed to be zero within this range and follows the egg-stage function under drier conditions – which is a conservative assumption, as juveniles are typically more drought-tolerant than eggs.

Adult temperature-dependent mortality is derived from full life-cycle studies (Roeben et al. 2023; Snider and Butcher 1973; Wehrli et al. 2024), where the daily death rate is calculated as the inverse of the interval between first oviposition and death. Soil-moisture-dependent mortality is inferred from chronic exposure experiments on adults (Wang et al. 2022; Wang et al. 2023), where mortality is measured only at the end of exposure. The daily death rate is therefore mortality divided by exposure duration.

Together, these adaptations reflect the limitations of available empirical data and the need for pragmatic modelling assumptions.

Framing the model

Domain of applicability

This model is designed to simulate population dynamics of *Folsomia candida* at spatial scales ranging from 100 to 1000 m^2, using daily time steps for simulations of up to five years. It explicitly represents eggs, juveniles, and adults and requires inputs for initial population density, daily soil temperature (top 7 cm), soil moisture (top 7 cm), and dimensionless food scores.

The model assumes linear effects of soil moisture on development from egg to juvenile and from juvenile to adult. Although non-linear effects may occur, current empirical data do not support more complex functions. The model also assumes no long-distance dispersal, and predation is implemented as a fixed consumption rate for all life stages. The predation rate is assumed to be constant, which might not be the case in reality. Additionally, food quality and availability are simplified as a score rather than mechanistic diet dynamics. It does not include explicit predator dynamics or long-term evolution (e.g., drought or heat tolerance). The model is explicitly tailored for *F. candida*, a parthenogenetic, opportunistic species with rapid reproduction under favourable conditions. It may be less representative of specialist or sexually reproducing springtails. However, with sufficient life-history data, the modelling framework could be adapted to other species.

Key biological processes not included

The model does not incorporate physiological acclimation, i.e., the reversible adjustment of physiology to prevailing temperature or soil moisture regimes, although acclimation can enhance stress tolerance in Collembola (Wehrli et al.

2024). All parameterisations use data from experiments in which specimens were not pre-acclimated to stress or sub-stress conditions.

Processes such as evolutionary adaptation and genetic variation are not included due to a lack of empirical data and the desire to avoid structural overcomplexity.

The model considers temperature and soil moisture intensively but only considers a rather simple food modelling. Although vegetation decomposition strongly influences available food resources, decomposition is not mechanistically linked to food score in the present version.

Philosophical boundaries

The model is built on a population-matrix framework with explicit spatial structure. Spatially explicit matrix models are uncommon and represent an innovation within development in modelling spatially distributed subpopulations (Duan and Topping 2024). The philosophical boundaries of the model arise from three main sources: the intrinsic limitations of matrix models, the assumptions embedded in the model design, and the constraints imposed by the ALMaSS framework with which it is integrated.

Because matrix models aggregate individuals into classes, this approach cannot capture individual variability arising from genetic or environmental heterogeneity, nor can it represent emergent behaviours that result from interactions among individuals. Furthermore, the use of thermal performance curves assumes that development is fundamentally predictable under given environmental conditions, potentially overlooking stochastic elements that contribute to population resilience, such as the interplay between individual health and developmental processes. Finally, the ALMaSS spatial framework further constrains environmental heterogeneity by assuming uniform conditions across each grid cell, thereby treating space as discrete rather than continuous.

Implication of model framing

Many exclusions in this formal model are not just a form of simplification but rather a balance between biological realism and data availability. The model is intended for exploring population-level consequences of multiple stressors in agricultural landscapes. Outputs include population growth rates, spatial distribution, equilibrium population size, or recovery of the population. These outputs should be interpreted as indicators of relative risk rather than absolute estimates of abundance. The model is thus primarily designed for comparing the relative impacts of different scenarios.

The EFSA Good Modelling Practice guidelines (2014) caution against modelling *F. candida* for use in the regulatory environmental risk assessment of plant protection products, as it does not represent natural soil communities well. However, this species remains highly relevant within ecotoxicological testing frameworks. *F. candida* is widely used in standardised laboratory and higher-tier tests (i.e., micro- or mesocosm experiments), including those conducted under environmentally realistic conditions, where it serves as a sensitive and well-characterised test organism. In this context, the model can be used to improve the interpretation and prediction of results of ecotoxicological experiments. This species is also found in agricultural and disturbed habitats

(Fountain and Hopkin 2005) and has been used as an indicator of soil quality (Nelson et al. 2011). With adaptation, the model could be extended to additional species with comparable ecology and available datasets.

Despite its integration within ALMaSS, the model can be implemented in any landscape modelling framework capable of supplying temperature, soil moisture, and soil classification data. The model structure is flexible and could be extended to incorporate elements such as explicit competition, predation, or pollutant exposure.

Acknowledgements

This work is part of the project SYBERAC, which is funded by the European Union as a Horizon Research and Innovation Action, Grant Agreement number 101135213. The authors thank Niels Holst for his comments on the model design.

References

Adhikari K, Hartemink AE, Minasny B, Bou Kheir R, Greve MB, Greve MH (2014) Digital mapping of soil organic carbon contents and stocks in Denmark. PLoS ONE 9(8): e105519. https://doi.org/10.1371/journal.pone.0105519

Adhikari K, Kheir RB, Greve MB, Bøcher PK, Malone BP, Minasny B, McBratney AB, Greve MH (2013) High-resolution 3-D mapping of soil texture in Denmark. Soil Science Society of America Journal 77(3): 860–876. https://doi.org/10.2136/sssaj2012.0275

Adhikari K, Minasny B, Greve MB, Greve MH (2014) Constructing a soil class map of Denmark based on the FAO legend using digital techniques. Geoderma 214: 101–113. https://doi.org/10.1016/j.geoderma.2013.09.023

Al-Kaisi M, Brun LJ, Enz JW (1989) Transpiration and evapotranspiration from maize as related to leaf area index. Agricultural and Forest Meteorology 48(1–2): 111–116. https://doi.org/10.1016/0168-1923(89)90010-5

Allen RG, Pereira LS, Raes D, Smith M (1998) Crop evapotranspiration - Guidelines for computing crop water requirements. FAO - Food and Agriculture Organization of the United Nations. https://doi.org/10.18356/fa70fd58-en

Bakonyi G (1989) Effects of *Folsomia candida* (Collembola) on the microbial biomass in a grassland soil. Biology and Fertility of Soils 7(2): 138–141. https://doi.org/10.1007/bf00292572

Booth RG, Anderson JM (1979) The Influence of Fungal Food Quality on the Growth and Fecundity of *Folsomia candida* (Collembola: Isotomidae). Oecologia (38): 317–323. https://doi.org/10.1007/bf00345191

Chiverton PA (1986) Predator density manipulation and its effects on populations of *Rhopalosiphum padi* (Hom.: Aphididae) in spring barley. Annals of Applied Biology 109: 49–60. https://doi.org/10.1111/j.1744-7348.1986.tb03183.x

Choi WI, Moorhead DL, Neher DA, Ryoo MI (2006) A modeling study of soil temperature and moisture effects on population dynamics of *Paronychiurus kimi* (Collembola: Onychiuridae). Biology and Fertility of Soils 43(1): 69–75. https://doi.org/10.1007/s00374-005-0062-5

Choi WI, Ryoo MI (2003) A matrix model for predicting seasonal fluctuations in field populations of *Paronychiurus kimi* (Collembola: Onychiuridae). Ecological modelling 162(3): 259–265. https://doi.org/10.1016/s0304-3800(02)00384-8

Curtin D, Beare MH, Hernandez-Ramirez G (2012) Temperature and moisture effects on microbial biomass and soil organic matter mineralization. Soil Science Society of America Journal 76(6): 2055–2067. https://doi.org/10.2136/sssaj2012.0011

Danish Agriculture Food Council (2000) Denmark - a Food and Farming Country Facts & Figures. https://doi.org/10.1080/01296612.2000.11727203

de Lima ESC, van Haren C, Mainardi G, de Rooij W, Ligtelijn M, van Straalen NM, van Gestel CAM (2021) Bringing ecology into toxicology: Life-cycle toxicity of two neonicotinoids to four different species of springtails in LUFA 2.2 natural soil. Chemosphere 263: 128245. https://doi.org/10.1016/j.chemosphere.2020.128245

Diekkrüger B, Röske H (1995) Modelling the population dynamics of *Isotoma notabilis* (Collembola) on sites of different agricultural usage. Pedobiologia 39(1): 58–73. https://doi.org/10.1016/s0031-4056(24)00164-1

Duan X, Topping CJ (2024) A general subpopulation model for the Animal Landscape and Man Simulation System (ALMaSS). Food and Ecological Systems Modelling Journal 5: e122467. https://doi.org/10.3897/fmj.5.122467

EFSA (2014) Scientific Opinion on good modelling practice in the context of mechanistic effect models for risk assessment of plant protection products. EFSA Journal 12(3). https://doi.org/10.2903/j.efsa.2014.3589

European Commission [EU Soil Strategy for 2030] (2021) Reaping the benefits of healthy soils for people, food, nature and climate. https://eur-lex.europa.eu/legal-content/EN/TXT/?uri=CELEX%3A52021DC0699

Fountain MT, Hopkin SP (2005) *Folsomia candida* (Collembola): a "standard" soil arthropod. Annual Review of Entomology 50: 201–222. https://doi.org/10.1146/annurev.ento.50.071803.130331

Frampton GK (1988) The effects of some commonly-used foliar fungicides on Collembola in winter barley: laboratory and field studies. Annals of Applied Biology 113: 1–14. https://doi.org/10.1111/j.1744-7348.1988.tb03276.x

Grégoire-Wibo C, Snider RM (1983) Temperature-related mechanisms of population persistence in *Folsomia candida* and *Protaphorura armata* (Insecta: Collembola). Pedobiologia (25): 413–419. https://doi.org/10.1016/s0031-4056(23)05950-4

Hersbach H, Bell B, Berrisford P, Biavati G, Horányi A, Muñoz Sabater J, Nicolas J, Peubey C, Radu R, Rozum I, Schepers D, Simmons A, Soci C, Dee D, Thépaut J-N (2023) ERA5 hourly data on single levels from 1940 to present. https://doi.org/10.24381/cds.adbb2d47

Hillel D (2003) Introduction to environmental soil physics. https://doi.org/10.1016/b978-0-12-348655-4.X5000-x

Holmstrup M (1994) Life history and growth of some soil living microarthropod species cultured in the laboratory.

Holmstrup M (2019) Water relations and drought sensitivity of *Folsomia candida* eggs (Collembola: Isotomidae). European Journal of Entomology 116: 229–234. https://doi.org/10.14411/eje.2019.025

Jensen TG, Holmstrup M, Madsen RB, Glasius M, Trac LN, Mayer P, Ehlers B, Slotsbo S (2020) Effects of alpha-pinene on life history traits and stress tolerance in the springtail *Folsomia candida*. Comparative Biochemistry and Physiology Part C 229: 108681. https://doi.org/10.1016/j.cbpc.2019.108681

Jia Q, Wang Y-P (2021) Relationships between leaf area index and evapotranspiration and crop coefficient of hilly apple orchard in the loess plateau. Water 13(14). https://doi.org/10.3390/w13141957

Johnson DL, Wellington WG (1983) Dispersal of the collembolan, *Folsomia candida* Willem, as a function of age. Canadian Journal of Zoology 61(11): 2534–2538. https://doi.org/10.1139/z83-335

Kaneda S, Kaneko N (2002) Influence of soil quality on the growth of *Folsomia candida* (Willem) (Collembola). Pedobiologia 46(5): 428–439. https://doi.org/10.1078/0031-4056-00150

Longstaff BC (1977) The dynamics of collembolan populations: a matrix model of single species population growth. Canadian Journal of Zoology 55(2): 314–324. https://doi.org/10.1139/z77-043

Meli M, Palmqvist A, Forbes VE (2014) Implications of interacting microscale habitat heterogeneity and disturbance events on *Folsomia candida* (Collembola) population dynamics: a modeling approach. Environmental Toxicology and Chemistry 33(7): 1508–1516. https://doi.org/10.1002/etc.2552

Nelson KL, Boiteau G, Lynch DH, Peters RD, Fillmore S (2011) Influence of agricultural soils on the growth and reproduction of the bio-indicator *Folsomia candida*. Pedobiologia 54(2): 79–86. https://doi.org/10.1016/j.pedobi.2010.09.003

Nielmeyer J (2022) Crop coefficient (Kc) estimation from leaf area index (LAI). In Science, Research & Data: Standford University.

Norouzi S, Pesch C, Arthur E, Norgaard T, Moldrup P, Greve MH, Beucher AM, Sadeghi M, Zaresourmanabad M, Tuller M, Iversen BV, de Jonge LW (2025) Physics-informed neural networks for estimating a continuous form of the soil water retention curve from basic soil properties. Water Resources Research 61(3): e2024WR038149. https://doi.org/10.1029/2024wr038149

OECD (2016) Test No. 232: Collembolan Reproduction Test in Soil. OECD Guidelines for the Testing of Chemicals, Section 2. https://doi.org/10.1787/9789264264601-en

Padfield D, O'Sullivan H (2023) rTPC: Fitting and Analysing Thermal Performance Curves. In (Version R package version 1.0.4) https://doi.org/10.32614/cran.package.rtpc

Petersen H (1994) A review of collembolan ecology in ecosystem context. Acta Zoologica Fennica 195: 111–118.

Petersen H, Luxton M (1982) A comparative analysis of soil fauna populations and their role in decompistion processes. Oikos 39: 287–388. https://doi.org/10.2307/3544689

Ponge J-F (2020) Move or change, an eco-evolutionary dilemma: The case of Collembola. Pedobiologia 79: 150625. https://doi.org/10.1016/j.pedobi.2020.150625

Ponge JF (1991) Food resources and diets of soil animals in a small area of Scots pine litter. Geoderma 49(1–2): 33–62. https://doi.org/10.1016/0016-7061(91)90090-g

R Core Team (2024) R: A Language and Environment for Statisitcal Computing. In R Foundation for Statisical Computing. https://doi.org/10.32614/r.manuals

Roeben V, Montoya-Tzschoppe L, Roß-Nickoll M (2023) Long life at low temperatures – The life-history of *Folsomia candida* at ecological relevant temperatures. Pedobiologia 96: 150847. https://doi.org/10.1016/j.pedobi.2022.150847

Rosso L, Lobry JR, Flandrois JP (1993) An unexpected correlation between cardinal temperatures of microbial growth highlighted by a new model. Journal of Theoretical Biology 162(4): 447–463. https://doi.org/10.1006/jtbi.1993.1099

Rusek J (1998) Biodiversity of Collembola and their functional role in the ecosystem. Biodiversity and Conservation 7(9): 1207–1219. https://doi.org/10.1023/A:1008887817883

Seastedt TR (1984) The role of microarthropods in decomposition and mineralization processes. Annual Review Of Entomology 29(1): 25–46. https://doi.org/10.1146/annurev.en.29.010184.000325

Snider RM, Butcher JW (1973) The life history of *Folsomia candida* (Willem) (Collembola: Isotomidae) relative to temperature. The Great Lakes Entomologist 6386: 1–10. https://doi.org/10.22543/0090-0222.1187

Talley SM, Coley PD, Kursar TA (2002) The effects of weather on fungal abundance and richness among 25 communities in the Intermountain West. BMC Ecology 2: 7. https://doi.org/10.1186/1472-6785-2-7

Thomsen P, Duan X, Topping CJ (2024) Formal model for *Acyrthosiphon pisum*, *Aphis fabae*, *Myzus persicae* and *Sitobion avenae* using the ALMaSS subpopulation approach. Food and Ecological Systems Modelling Journal 5: e123747. https://doi.org/10.3897/fmj.5.123747

Topping CJ, Kondrup Marcussen L, Thomsen P, Chetcuti J (2022) The Formal Model article format: justifying modelling intent and a critical review of data foundations through publication. Food and Ecological Systems Modelling Journal 3: e91024. https://doi.org/10.3897/fmj.3.91024

van Amelsvoort PAM, Usher MB (1989) Egg production related to food quality in *Folsomia candida* (Collembola: Isotomidae): effects on life history strategies. Pedobiologia 33(1): 61–67. https://doi.org/10.1016/s0031-4056(24)00183-5

Wang Y, Slotsbo S, Damgaard CF, Holmstrup M (2023) Influence of soil moisture on bioaccumulation, growth, and recruitment of *Folsomia candida* Exposed to phenanthrene-polluted soil. Environmental Science & Technology 57(8): 3085–3094. https://doi.org/10.1021/acs.est.2c07497

Wang Y, Slotsbo S, Holmstrup M (2022) Soil dwelling springtails are resilient to extreme drought in soil, but their reproduction is highly sensitive to small decreases in soil water potential. Geoderma 421. https://doi.org/10.1016/j.geoderma.2022.115913

Wehrli M, Slotsbo S, Fomsgaard IS, Laursen BB, Groning J, Liess M, Holmstrup M (2024) A dirt(y) world in a changing climate: Importance of heat stress in the risk assessment of pesticides for soil arthropods. Global Change Biology 30(10): e17542. https://doi.org/10.1111/gcb.17542

Wehrli M, Slotsbo S, Ge J, Holmstrup M (2024) Acclimation temperature influences the thermal sensitivity of injury accumulation in *Folsomia candida* at extreme low and high temperatures. Current Research in Insect Science 6: 100089. https://doi.org/10.1016/j.cris.2024.100089

Wei T, Simko V (2021) R package 'corrplot': Visualization of a Correlation Matrix. In (Version Version 0.92). https://doi.org/10.32614/cran.package.corrplot

Wickham H (2016) ggplot2: Elegant Graphics for Data Analysis. In Springer-Verlag. https://doi.org/10.1007/978-0-387-98141-3

Xie L (2023) Multiple Stressors in "COLLEMBOLAND": Assessing the Effects of Multiple Stressors on Collembola at the Individual and Extrapolate to the Population-level Aarhus University]. Aarhus, Denmark.

Xie L (2026) Data and scripts for the paper of Integrating spatial and environmental stressors in a population model of *Folsomia candida* (Collembola: Isotomidae): a Formal Model within ALMaSS framework [Dataset]. Dryad. https://doi.org/10.5061/dryad.69p8cz9hk

Xie L, Slotsbo S, Ilyaskina D, Forbes V, Holmstrup M (2024) Chronic effects of an insect growth regulator (teflubenzuron) on the life cycle and population growth rate of *Folsomia candida*. Environmental Toxicology and Chemistry 43(5): 1173–1183. https://doi.org/10.1002/etc.5850

Ziółkowska E, Bednarska A, Laskowski R, Topping C (2023) The Formal Model for the solitary bee *Osmia bicornis* L. agent-based model. Food and Ecological Systems Modelling Journal 4: e102102. https://doi.org/10.3897/fmj.4.102102

Supplementary material 1

Additional information

Authors: Liyan Xie, Xiaodong Duan, Sarem Norouzi, Lis Wollesen de Jonge, Christopher J. Topping

Data type: docx

Copyright notice: This dataset is made available under the Open Database License (http://opendatacommons.org/licenses/odbl/1.0/). The Open Database License (ODbL) is a license agreement intended to allow users to freely share, modify, and use this Dataset while maintaining this same freedom for others, provided that the original source and author(s) are credited.

Link: https://doi.org/10.3897/aem.8.184962.suppl1

Additional information

Conflict of interest

The authors have declared that no competing interests exist.

Ethical statement

No ethical statement was reported.

Artificial Intelligence (AI) use

The authors accept full responsibility for the content of the manuscript, including the disclosure of any use of AI.
No AI tools were used in the preparation of this manuscript.

Funding

This work is funded by the European Union as a Horizon Research and Innovation Action, Grant Agreement number 101135213.

Author contributions

Conceptualization: LX, CJT. Data curation: LWJ, LX, SN. Formal analysis: CJT, LX, LWJ, XD, SN. Funding acquisition: CJT. Investigation: LX, XD. Methodology: XD, CJT, LX. Supervision: CJT. Visualization: LX. Writing - original draft: LX. Writing - review and editing: LX, CJT, XD, SN, LWJ.

Author ORCIDs

L. Xie https://orcid.org/0000-0002-6154-5165
X. Duan https://orcid.org/0000-0003-2345-4155
S. Norouzi https://orcid.org/0000-0003-2255-8657
L.W. de Jonge https://orcid.org/0000-0003-2874-0644
C.J. Topping https://orcid.org/0000-0003-0874-7603

Data availability

The data underpinning the analysis reported in this paper are deposited at Dryad (Xie 2026). Model fitting was performed in R Studio (Version 4.4.2) (R Core Team 2024). Thermal performance curves were fitted using the rTPC package (Padfield and O'Sullivan 2023). Visualisation of fitted functions used the corrplot and ggplot2 packages (Wei and Simko 2021; Wickham 2016).